Finite Element Vibration Analysis and Modal Testing of Bells

Jahangir Ansari
Virginia State University
Engineering and Technology Learning Center
jansari@vsu.edu

Abstract

When bells are manufactured by traditional methods**,** the ideal symmetries are usually all broken due to irregularity of shape, material properties, and local defects during the casting process. Therefore, the vibration analysis of bell type structures become complicated and sometimes predicting precise results is not possible. Lack of generalized mathematical representation of bell vibrations necessitates numerical and/or experimental methods to determine the vibration characteristics of these types of structures.

Rapid advances in computer aided design and manufacturing technology, as well as the accuracy of the virtual instrumentation programs in recent years, cause the possibility of solving such complex vibration problems. In this study a finite element commercial package is used for vibration analysis. Modal simulation and LabView are used as well for experimental measurements of the first five natural frequencies.

As an initial step toward more sophisticated situations and in order to reduce the complexity of the problem, the variation of the wall thickness only in the region of the soundbow is considered. Moreover, damping of any kind is neglected. The effect of the wall thickness (particularly *soundbow* thickness) on the first five musical modes is studied in detail. The experimental modal parameters obtained by impact testing were compared with corresponding analytical results obtained by the finite-element analysis.

Introduction

In practice, bells are imperfect and the ideal symmetries are usually broken due to irregularity of shape, material properties, and local defects during the casting process. Therefore, the vibration analysis of bell type structures becomes complicated and sometimes prediction of precise results is not easily possible. Lack of generalized mathematical representation of bell vibrations necessitates numerical and/or experimental methods to determine the vibration characteristics of these types of structures. Various experimental methods have been used by some authors to study the complex vibrations of bells [1, 2]. Using Finite Element Method and/ or modal testing, the vibration characteristics of both western and oriental bells are found in practice [3]. In this study the effect of wall thickness on the natural frequencies and corresponding mode shapes are discussed.

The present discussion of the vibration characteristics of bells are divided into two parts. The experimentally predicted results and the results obtained by finite element modeling of a bell are discussed in this paper. The practical modifications done on the bell to obtain the desired beating and modal characteristics are under study and will be discussed in a companion paper in the future.

Theoretical Background

A simple theoretical starting point is to approximate the bell as a cylindrical shell to estimate the basic geometry. The natural frequencies and corresponding radial displacements of a hinged cylindrical shell with a being the radius, L the length, and h the thickness, can be obtained from the following inextensional approximation [4] derived by Rayleigh [5]:

$$\omega_{mn} = \sqrt{\frac{E}{12\rho\,(1-\mu^2)}}\,(\frac{h}{a})\;\frac{1}{a}\;[(m\pi\;\frac{a}{L})^2 + n^2] \tag{1}$$

$$u_{mn} = A\sin(\frac{m\pi\,x}{L})\cos n(\theta\;-\phi\;)e^{j\omega t} \tag{2}$$

Where; E, ρ and μ are Young's modulus, mass density and Poisson's ratio of shell material, respectively.
As it can be seen from equation (1), in the preliminary design stage sufficient information can be obtained. By pre-selecting the fundamental natural frequency, the main geometry of the bell can be easily determined. But for detail design it is not possible to apply a parametric equation to get all the required design information. Therefore, using numerical methods such as Finite Element modeling is necessary to analyze the problem. As it can be seen from equation (1), natural frequencies can be controlled by controlling the shell thickness, radius to length ratio and the radius itself. By having in mind that the radius to length ratio of bells is approximately between1.1 to 1.4, equation (1) can be used successfully for estimating the fundamental natural frequencies in the preliminary design stages. Next, control can be done by thickness of the *Soundbow*, where the thicker Soundbow results in higher natural frequencies. In higher natural frequencies the effect of the Soundbow thickness becomes more noticeable.

Finite Element Modeling

The equation of motion of a system under conservative loading can be derived from the well-known Hamilton's Variational Principle. Hamilton's principle states that the actual path followed by a dynamic process is:

$$\delta\;H\; = \int_{t_0}^{t_1} \delta\;(U_E - K_E - W_E)\;\;dt = 0 \tag{3}$$

Where U_E, K_E and W_E are strain energy, kinetic energy and work done by applied external forces respectively. For a thin elastic shell, the variation in strain energy is given by:

$$\delta U_E = \int_A \{N\}^T \delta \{\varepsilon\} \, dA \tag{4}$$

The stress resultants and stress couples are related to the middle surface strains and curvature changes through an elastic matrix by:

$$\{N\} = \lfloor E \rfloor \{\varepsilon\} \tag{5}$$

Matrix $[E]$ contains both bending stiffness $D = Eh^3/12(1-\upsilon^2)$ and extensional stiffness $C = Eh/(1-\upsilon^2)$ of the element.

In order to facilitate the satisfaction of displacement continuity in an assemblage of the shell elements, the generalized displacements $\{q\}$ must be used in for degrees of freedom on nodes. Therefore, using Eq.(4) the variation in strain energy for an element becomes:

$$\delta U_E = \{q\}^T [k] \delta \{q\} \tag{6}$$

$[k]$ is known as the stiffness matrix of the element. The variation in kinetic energy for an element can be found as:

$$\delta K_E = \left\{q\right\}^T [m] \delta \left\{\overset{\circ\circ}{q}\right\} \tag{7}$$

Substituting equations (6) and (7) in equation (3) and summing for all the ***n*** elements comprising the original structure, after simplification the variation equation becomes

$$\sum_{i=1}^{n} \left\{ \int_{t_0}^{t_1} \delta \{q_i\}^T [[k_i] \{q_i\} + [m_i] \left\{\overset{\circ\circ}{q_i}\right\} - \{F_i\}] \, dt \right\} = 0 \tag{8}$$

Since equation (8) is valid for any arbitrary variation $\delta \{q_i\}^T$ the vanishing of the coefficient leads to the equations of motion

$$[K]\{q\} + [M]\left\{\overset{\circ\circ}{q}\right\} = \{F\} \tag{9}$$

Where $[K]$ and $[M]$ are stiffness and mass matrices for the entire shell respectively and $[F]$ is the total generalized force.

Once the finite element model is completely defined, the element stiffness and mass matrices, and then the resonance frequencies and corresponding mode shapes are computed.

Experiment Setup for Impact Excitation

Impact excitation is used in this study to predict the natural frequencies of the bell specimen. The bell shown in Figure 1 cast from brass is used for vibration testing and modal analysis. National Instruments' LabVIEW 7.1 software and National Instruments' PCI-4474 data acquisition board are used for data collection. The system collects signals from the impulse hammer (Omega's IH-101) and the accelerometer (Omega's ACC104A) attached to the outside surface of the bell rim.

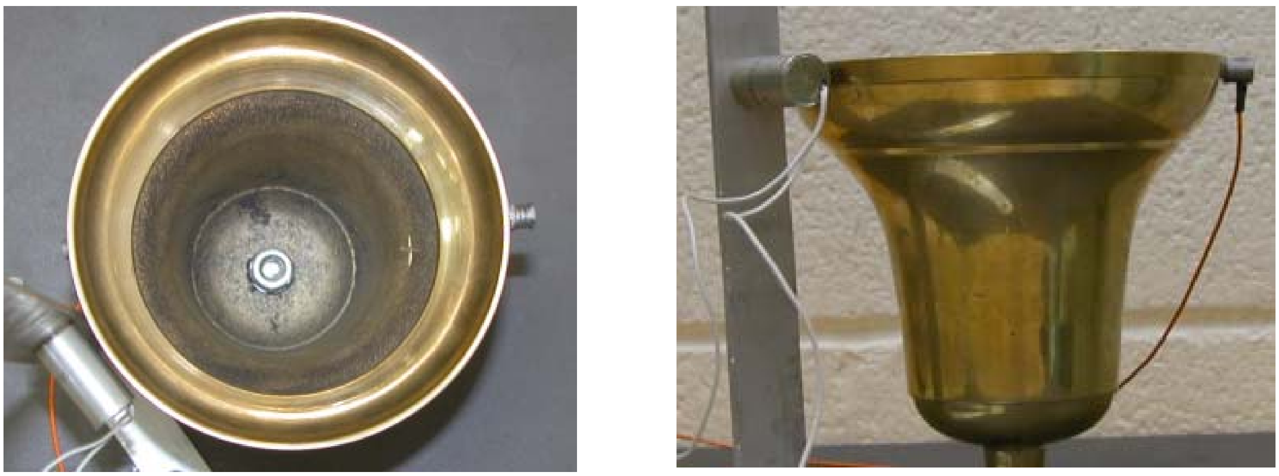

Figure 1: Bell specimen used for Impulse Excitation

By striking the specimen at any point on its surface and displaying the response signals from the accelerometer in the frequency domain, the fundamental natural frequencies can be measured at resonant peaks. To illustrate the normal mode shapes corresponding to natural frequencies, the Fast Fourier Transform of signals from both impulse hammer and accelerometer should be analyzed to find the transfer function of the system. In general, such transfer function describes the complex ratio of a resultant motion signal from the accelerometer divided by an exciting force signal from the impulse hammer. By using the amplitude (gain) and the phase difference of a transfer function at peak points, the damping factors can be accurately measured. The gain is usually expressed in dBs (decibels) with level of zero corresponding to an output level being equal to input signal. Phase difference is expressed in degrees, and it represents the lead or lag of the output signal with respect to the input signal of the system.

Striking the specimen at several points on a circumference and collecting the gain values and corresponding phase difference signs for a resonance frequency will provide data for graphing lateral mode shape for that frequency [6]. It should be noted that since the gain values are in dBs, it is necessary to calculate the linear units by applying the following formula:

$$Y = (10)^{dB/20}$$

Frequency Analysis

Time domain voltage signals of the accelerometer and impulse hammer for a sample test are shown in Figure 2. The duration of the impulse signal is less than 10 ms. The accelerometer signal has 1mV peak-to-peak and decreases gradually. This figure illustrates that the recording time of 0.1 sec is enough to store the meaningful data.

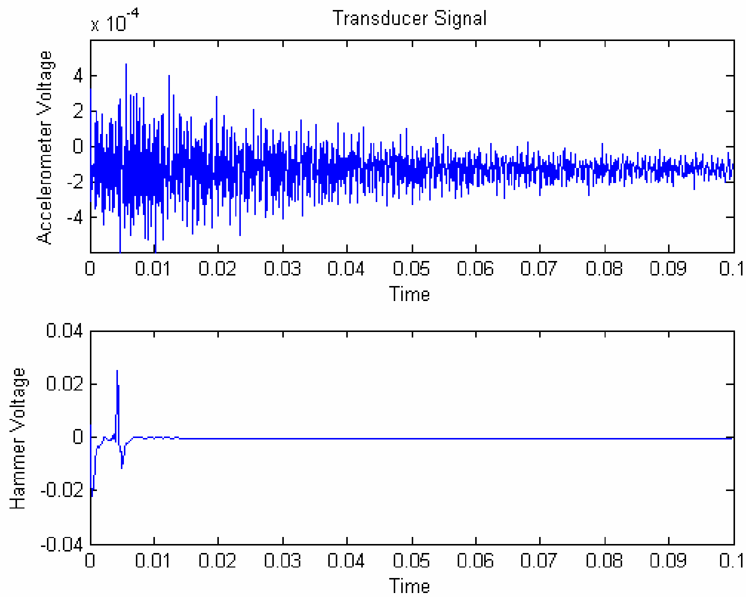

Figure 2: Voltage Signals in Time Domain

The fundamental natural frequencies of the model can be predicted from the frequency domain of the accelerometer response. The bell was excited from different positions and the predicted frequencies were almost the same in all cases. Figure 3 illustrates how the accelerometer responses in frequency domain for two different excitations.

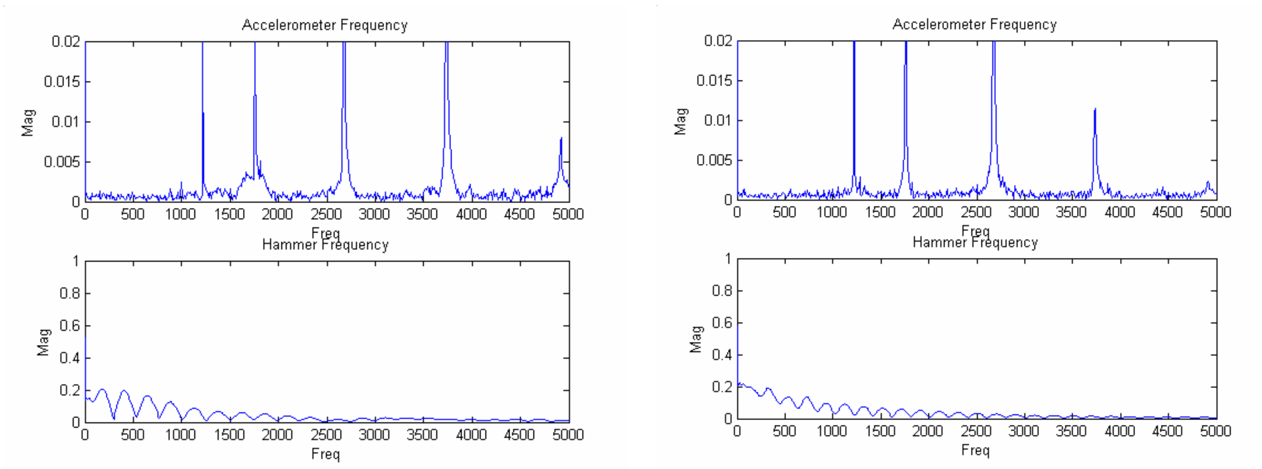

Figure 3: Frequency Responses of Accelerometer

To determine the circumferential mode shape corresponding to a natural frequency of the model, a large number of repeated tests are required. Fixing the accelerometer on the bell soundbow, striking the model at different points on the same circumference, and using transfer functions will show how the stroked points will be deflected relative to the accelerometer's position. Figure 4 illustrates the transfer functions of the amplitude and phase for a sample test.

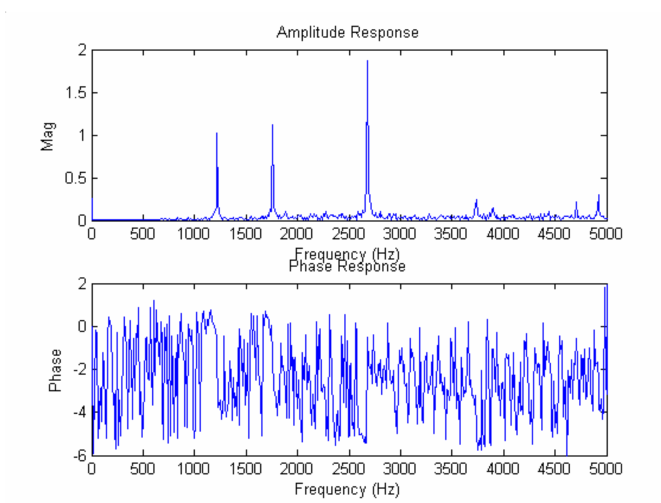

Figure 4: Transfer Functions of Amplitude and Phase

The analysis of captured signals from accelerometer responses and transfer functions gives the same five natural frequencies of the model shown in Table 1.

Table 1: Natural frequencies of the model (Experiment)

Frequencies Hz	1220	1760	2680	3745	4935
Ratio to the First mode	1.00	1.44	2.20	3.07	4.05

FE Analysis

A commercial FEA package was used to find the natural frequencies and corresponding mode shapes of the model. The thickness of the model varied from 0.06 in. at open side (sound bow) region, to 0.15in. at the close side (hanger) region. The material properties of the specimen used for analysis are shown in Table 2.

Table 2: Material Properties of the Specimen

Young's modulus (E)	16.7 E6	lb/in^2
Density	0.32	lb/in^3
Poisson's ratio	0.3	

In this study, the model was meshed into 4360 quadratic elastic shell elements with 13,157 degrees of freedom. The profile geometry and generated finite elements of the model are shown in Figure 5.

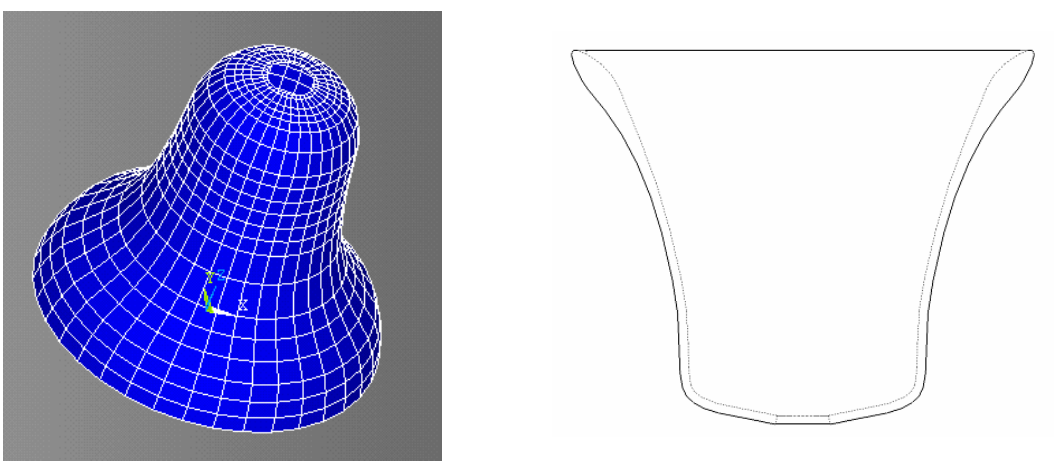

Figure 5: The profile geometry and generated finite elements of the model

The FE analysis was done to find the targeted eigen frequencies and corresponding eigen modes. The graphical results for the first four predicted lateral resonance frequencies and corresponding mode shapes are illustrated in Figure 6.

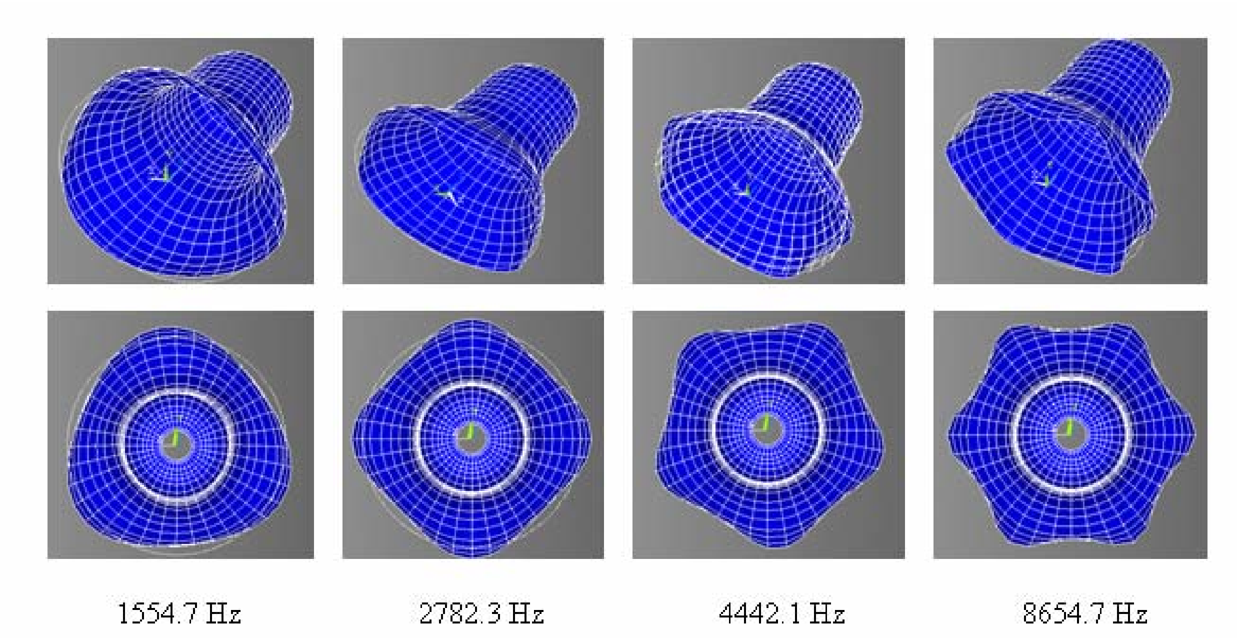

Figure 6: Fundamental Frequencies and Corresponding Mode Shapes by FEA

Results and discussion

Figure 8 shows the harmonics mode shapes for the first four lateral vibration modes. These are the 3rd, 4th, 5th, and 6th harmonics mode shapes. The ratial relationships of these frequencies lead to the estimated 2nd harmonic frequency being 1530.5 Hz. This is shown in table 3.

Table 3: Natural frequencies of the first mode vibration (FEM)

First Mode Vibration (one circumference node)	Harmonic number				
	2	3	4	5	6
Frequencies Hz	***1391.15****	1554.7	2782.3	4442.1	8654.7
Frequency Ratio	1.00	1.12	2.00	3.19	6.22
***** This frequency was estimated					

Even though comparisons of Tables 1 and 3 show close agreements between the two results, additional experiments are yet needed for comparing the individual vibration modes. The study may continue to include the prediction of the mode shapes for each natural frequency.

Conclusion

Comparison between the results from analytical and experimental results shows good agreements for the resonance frequencies in most cases. Increasing the bell thickness in the soundbow region causes the resonance frequencies to be slightly increased in higher modes. Bells having thicker soundbow have the tendency of suppressing normal displacements of the open edge. Since it is not certain that the mode shapes appear for the corresponding frequencies of the analytical and experimental results are same, therefore, the next step should be experimental prediction of mode shapes of higher resonance frequencies.

In the course of a further investigation, the effect of irregularity (such as a crack) along a meridian on the modal and beat characteristics of a bell should be studied as well.

Bibliography

1. Herbert L. Kuntz and Elmer L. Hixson, 1986, "Vibration characteristics of two bouy bells," J. Acoust. Soc. Am. 79(6), June 1986, pp. 2012-2020.
2. T. D. Rossing and H. J. Sathoff, "Modes of vibration and sound radiation from tuned handbells," J. Acoust. Soc. Am. 68, 1980, pp. 1600-1607.
3. J. Ansari, Yung-Ha Yum, Jang Moo Lee, 1985, "A Study on the Vibrations of Axisymmetric Shells," Proceeding of the 3rd International Modal Analysis Conference, pp. 1138-1144.
4. W. Soedel, 1993, "Vibration of Shells and Plates" Marcel Dekker.
5. Lord Rayleigh (j. W. Strutt), The Theory of Sound (Macmillian, London, 1894), Vol. I (reprinted by Dover, 1945).
6. Steve Goldman, "Vibration Spectrum Analysis", Industrial Press, Inc. ISBN 0-8311-3088-1.